

## Tribological Aspects of the Process of Winding the Steel Rope Around the Winch Drum

M. Matejić<sup>a</sup>, M. Blagojević<sup>a</sup>, V. Marjanović<sup>a</sup>, R. Vujanac<sup>a</sup>, B. Simić<sup>b</sup>

<sup>a</sup> Faculty of Engineering, University of Kragujevac, Serbia.

<sup>b</sup> D.O.O RAPP Zastava, Serbia.

### Keywords:

Winch  
Drum  
Rope  
Friction  
Friction force

### ABSTRACT

Proper winding of the steel rope around the winch drum is great importance, mostly for: prolonging the service life of the rope, reduction of deformations of the body and the sides of the drum if the winding of the rope is multilayered, increasing of the safety factors, easier unwinding of the rope while lowering the load, even running of the drive unit, etc. The focus of this paper is on the analysis of the friction which occurs in the process of winding and unwinding the rope around the winch drum. Friction force is in its highest intensity when the rope passes from one layer to another, if the winding of the rope is multilayered. As the result of the research, certain mechanisms of winding of the rope from the aspects of the friction force were obtained, and the effects of the forces on the sides of the drum were analyzed.

### Corresponding author:

M. Matejić  
Faculty of Engineering,  
University of Kragujevac,  
Serbia.  
E-mail: mmatejic@kg.ac.rs

© 2014 Published by Faculty of Engineering

## 1. INTRODUCTION

Modern technological achievements have enabled a great progress in the ship equipment industry. Ship winches, as one of the most important parts of the equipment, are highly developed. Their dimensions, compared to the force they use, have been reduced and the degree of efficiency has increased with the use of various kinds of compact mechanical gear and drive. The capacities for winding of the ropes have been increased for any kind of use on the vessels, from the oceanographic researches on the bottom of the ocean, to catching of the special kinds of fish.

A lot of research into vessel winches have been done: increasing of the degree of efficiency,

reduction of dimensions, reduction of the mass of winches, improvement of the drive unit regarding the compactness and the power they use, improvement of the drum for rope-winding as the basic element of a winch, of the rope-winding system, development and analysis of the various types of ropes for various uses, etc.

Great attention is paid to examination and development of the ropes used for winches. Steel ropes are mostly used for vessel winches, while the synthetic ones are rarely used. Different types of cables are used for winches for oceanographic researches rather than ropes because of the transmission of information from the research devices from the bottom of the ocean to the vessel. When it comes to the development of the new types of ropes, great

attention is paid both to the outer tensile and twisting forces affecting the rope, and the inner friction forces that occur between the wires of the rope, [1-3]. Various types of materials in different conditions are considered in setup of the problem, [4-6]. When examining the existing types of ropes, it is very important to examine the inner friction in the ropes, as well as the failure mechanism of the ropes, [7, 8]. In the case where the steel rope cannot be installed on a winch because of its large mass, synthetic ropes are used. Synthetic ropes are still not widely used because they are still in the development and improvement stages, [9]. Synthetic ropes can be made with the molten core for the improvement of its mechanical characteristics.

Reduction of the dimensions and the increase in the degree of efficiency of a winch is mostly achieved by installing the compact mechanical gear, gearboxes. Single-stage gearboxes with two, three or more drives are often used for increasing the compactness of the vessel winch constructions, [10]. In addition, the use of planetary gearboxes is common for their ability to be installed within the winch drum.

Improvement of the winch drum, as the basic element of the winch, is based on the examination of the effect of the forces on the drum, experimentally and using finite element analysis, [11]. Improvement of the drum is done by reducing the thickness of the material from which the drum is made in noncritical places, while increasing it in the critical ones, and inserting the required structural stiffeners, [12, 13]. Optimization methods are also a possible approach of improvement, [14].

Improvement of the system for proper winding of the rope around the drum of the vessel winch is based on its synchronization with the number of turns of the drum. The synchronization can be done in many ways. Some of the ways are the mechanical synchronization with the power transmission or installing a special driving engine-generator for the system, which is synchronized, with the engine-generator of the winch.

In this paper, a mathematical model of winding of a steel rope around the drum is presented. The mathematical model shows the correlation between the friction and pulling forces using

geometrical characteristics of winding on the winch drum and the friction coefficient. Following this, the results of the algorithm, which are also developed in this paper, mathematical model as well as comparison characteristics of friction forces for different coefficients of friction during winding, are given. Finally conclusions and guidelines for further research have been presented.

## 2. MATHEMATICAL MODEL OF STEEL ROPE WINDING AROUND THE WINCH-DRUM

The winding of the steel rope around the winch drum can be single-layered or multilayered. The mathematical model concerns the multilayered process of rope winding, from the first to the last layer. The model could be used for defining single-layered winding too, by excluding the upper layers from the model. The bevel of the rope due to the winding is excluded from the mathematical model, because the bevel has an insignificant effect in the majority of winding cases. Also, the assumption that during winding the rope acts as an absolute elastic body is taken, while the wound rope acts as a solid body.

### 2.1 General case of winding of the rope around the drum

In determining the general case of winding, an  $n$ th winding on the  $n$ th layer is observed. The winding lies upon the two windings from the previous layer (Fig. 1).

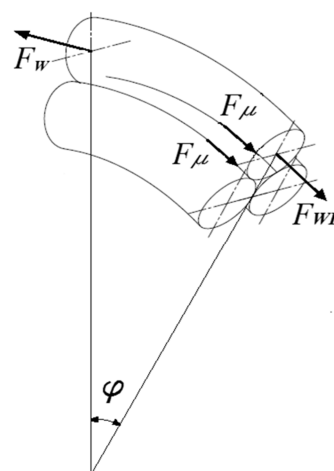


Fig. 1. General spooling case.

The forces  $F_{WR}$  occur as the reaction of the rope to the pulling force  $F_w$ . The friction force  $F_{\mu}$  also

occurs. Further observation is done on the cross-section where the force  $F_{WR}$  acts (Fig. 2). In this cross-section, the perpendicular force  $F_N$  occurs due to acting of friction force  $F_\mu$ .

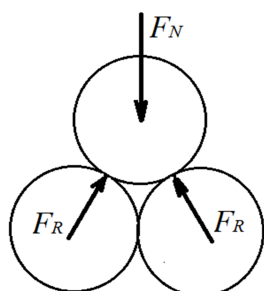


Fig. 2. Cross-section of ropes in general case.

Since the rope is of constant cross-section, the centers of circumferences, which make the cross-section of the rope, generally, form an equilateral triangle. Horizontal component reaction forces of the windings of the lower layer  $F_R$  are annulled because of the previous claim. The connection between the perpendicular force  $F_N$  and the reaction force  $F_R$  is derived by setting the planar system of opposed forces, and the resulting is relation (3):

$$F_R = \frac{F_N \sqrt{3}}{3} \quad (1)$$

After determining the reaction, it is necessary to determine the friction force, which is caused by the tractive force. The friction force was determined by observing the simplified tensile system of the upper layer of rope over the lower layer (Fig. 3) on a small angle  $\pm d\varphi/2$  from the cross-section shown on the Fig. 2.

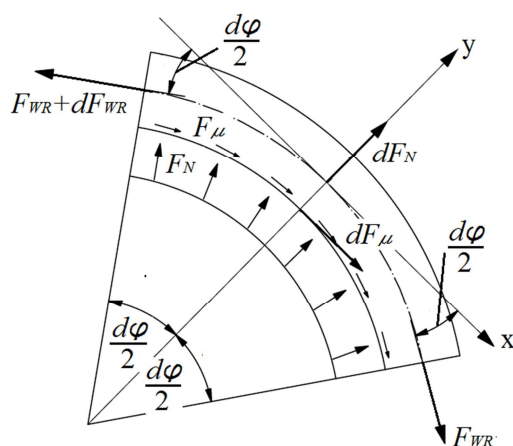


Fig. 3. Basic part of the rope.

For the elementary part of the rope on the angle  $\pm d\varphi/2$ , the following equation system is derived:

$$x : dF_\mu - (F_{WR} + dF_{WR}) \cos \frac{d\varphi}{2} + F_{WR} \cos \frac{d\varphi}{2} = 0 \quad (2)$$

$$y : dF_N - (F_{WR} + dF_{WR}) \sin \frac{d\varphi}{2} - F_{WR} \sin \frac{d\varphi}{2} = 0 \quad (3)$$

Accepting the assumptions for the basic angle  $\pm d\varphi/2$  ( $\varphi \rightarrow 0$ ):  $\cos d\varphi/2 \approx 1$ ,  $\sin d\varphi/2 \approx d\varphi/2$ ,  $dF_\mu = \mu \cdot dF_N$  i  $dF_{WR} d\varphi = 0$ , and by solving equations (2) and (3), the connection between the inputted pulling force  $F_W$  and the reaction force within the rope  $F_{WR}$ :

$$F_W = F_{WR} \cdot e^{\mu\varphi} \quad (4)$$

With further solving, the connection between the tractive force  $F_W$  and perpendicular force  $F_N$  is obtained, as well as the connection between the friction force  $F_\mu$  and the tractive force  $F_W$ :

$$F_N = \frac{F_W}{\mu} \left( 1 - \frac{1}{e^{\mu\varphi}} \right) \quad (5)$$

$$F_\mu = F_W \left( 1 - \frac{1}{e^{\mu\varphi}} \right) \quad (6)$$

From expressions (4), (5) and (6) it can be seen that all resulting values directly depend on the tractive force  $F_W$ , coefficient of friction  $\mu$ , and the angle of winding  $\varphi$ .

Returning the values from expression (5) to expression (1) the function of the reaction of the rope on the lower layer (7) is derived depending on the tractive force, coefficient of friction, and the angle of rope winding:

$$F_R = \frac{\sqrt{3}}{3} \frac{F_W}{\mu} \left( 1 - \frac{1}{e^{\mu\varphi}} \right) \quad (7)$$

The friction force  $F_\mu$  in the expression (6) was calculated as the total friction force. Because of the adopted assumption about the symmetry of winding, the friction force  $F_\mu$  is divided into two equal parts (8) (Fig. 1) in order to make a relation between the friction force appearing in the contact of the upper and lower layers.

$$F_{\mu_{LC}} = \frac{F_W}{2} \left( 1 - \frac{1}{e^{\mu\varphi}} \right) \quad (8)$$

## 2.2 Special case of rope winding on the drum

In the special case of rope winding on the drum (Fig. 4), the crossover of the rope from layer  $n$ th to the  $n$ th+1 layer is considered. The critical wind is observed in this case, during the

crossover. In this case, in the beginning, the contact on the last wind of the previous lower layer and the side of the drum occurs, while in the second wind that contact is lost, and the rope changes to the general winding case.

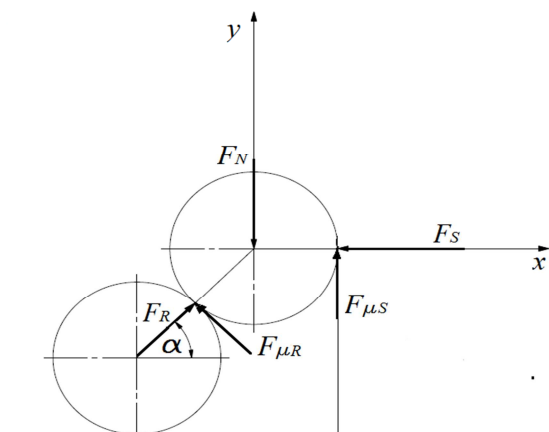


Fig. 4. Special rope winding case.

Establishment of the connection between the forces of reaction of the lower layer of the rope  $F_R$ , of friction between the layers of the rope  $F_{\mu R}$  ( $F_{\mu R} = F_R \cdot \mu_2$ ), forces of reaction on the side  $F_{\mu S}$  ( $F_{\mu S} = F_S \cdot \mu_1$ ) and perpendicular force  $F_N$ , in this case must be done by introducing the angle  $\alpha$ . This changes in the interval of  $0 \leq \alpha \leq \pi/2$ , while the angle of the winding changes in the interval of  $0 \leq \varphi \leq 2\pi$ . The connection between angle  $\alpha$  and the angle of winding  $\varphi$  is established according to the fact that for the angle  $\varphi = 2\pi$  [rad] the rope is winding for the length of the diameter of the rope  $d_w$ , while angle  $\alpha$  changes from 0 to  $\pi/2$ .

$$x: F_R \cos \alpha - \mu_2 \cdot F_R \sin \alpha - F_S = 0 \quad (9)$$

$$y: F_R \sin \alpha + \mu_2 \cdot F_R \cos \alpha - F_N + \mu_1 \cdot F_S = 0 \quad (10)$$

By solving the equations above the following expressions are obtained:

$$F_R = \frac{F_N}{(1 - \mu_1 \mu_2) \sin \alpha + (\mu_1 + \mu_2) \cos \alpha} \quad (11)$$

$$F_{\mu R} = \frac{\mu_2 F_N}{(1 - \mu_1 \mu_2) \sin \alpha + (\mu_1 + \mu_2) \cos \alpha} \quad (12)$$

$$F_S = \frac{F_N (\cos \alpha - \mu_2 \sin \alpha)}{(1 - \mu_1 \mu_2) \sin \alpha + (\mu_1 + \mu_2) \cos \alpha} \quad (13)$$

$$F_{\mu S} = \frac{\mu_1 F_N (\cos \alpha - \mu_2 \sin \alpha)}{(1 - \mu_1 \mu_2) \sin \alpha + (\mu_1 + \mu_2) \cos \alpha} \quad (14)$$

In the expressions (11), (12), (13) and (14) the friction coefficient  $\mu_1$  is the friction coefficient between the rope and the drum of the winch,

while  $\mu_2$  is the friction coefficient between the windings of the rope.

### 3. FRICTION FORCES IN THE WINDING OF THE STEEL ROPE AROUND THE WINCH DRUM

For this paper a mathematical model has been developed which for given initial parameters of winding of the rope gives the friction forces diagrams, perpendicular forces, as well as the comparative friction forces diagram for different coefficients of friction. The initial parameters according to which the forces were calculated are given in Table 1.

Table 1. Initial parameters for force examination.

Size description	Designation	Value
Drum length	$L$	100 [mm]
Wire diameter	$d_w$	10 [mm]
Number of winded layers	$n_L$	10
Load weight	$m$	250 [kg]
Friction coefficient	$\mu_1$	0,25
Friction coefficient	$\mu_2$	0,35

Mathematical model for calculating the force values has been developed in *MS Excel* software. The division of the winding angle was made with  $10^\circ$ , but was converted to radians for easier clarification. All of the output diagrams have the division in radians [rad] on their  $x$  - axis, and in Newtons [N] on the  $y$  - axis.

#### 3.1 Spooling of the rope on the first layer

In the spooling of the first layer it is characteristic that the friction force occurs only on one rope inlet. Because of the relatively small friction coefficient ( $\mu_1 = 0,25$ ) during the first layer spooling, the friction force  $F_{\mu}$  does not have a rapid increase in the first two layers ( $\varphi \approx 18$  [rad]) regarding the greater friction coefficients (Fig. 5).

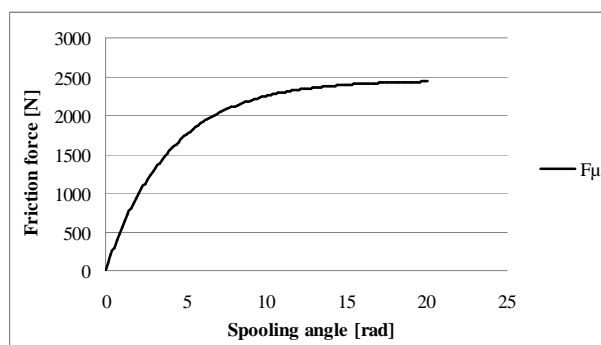
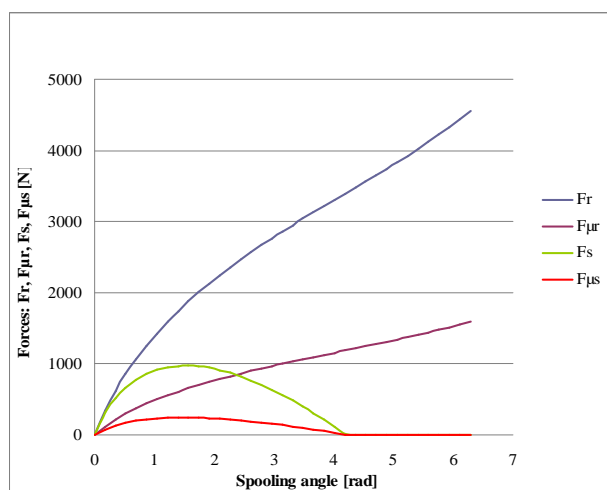


Fig. 5. Friction force  $F_{\mu}$  on the first layer dependence on the spooling angle.

At the end of the third layer spool ( $\varphi \approx 18$  [rad]), the friction force is almost equal to the pulling force. It can be said with certainty that after the fourth spool, with the friction coefficient being  $\mu_1 = 0,25$ , the whole load of tractive force is carried by the friction force.

### 3.2 Rope spooling in the crossover from one layer to another

The rope spooling is most critical in the crossover from one layer to another (Fig. 6). In that case, only one critical winding is observed during the crossover from layer  $n$  to layer  $n + 1$ , until the rope turns to the general spooling case. In this case, it is very hard to determine the friction coefficient between the winding spool and the last spool on the previous layer because of the changing trajectory of the rope inlet. When the rope gets to this position, the friction force appears in the contact between the side of the drum and the spool that is being wound by the rope inlet, but also the friction force appears in the contact between the last spool on the previous layer and the spool being wound. In this case, the assumed coefficient of friction which occurs in the rope inlet is the same as the friction coefficient which occurs between the rope spools ( $\mu_2 = 0,35$ ).



**Fig. 6.** The reaction force of the lower rope layer  $F_R$ , friction force between the rope layers  $F_{\mu R}$ , reaction force on the side  $F_S$  and friction force on the side  $F_{\mu S}$  dependence on the spooling angle.

From the diagram on the Fig. 6 which shows: the reaction force of the lower rope layer  $F_R$ , friction force between the rope layers  $F_{\mu R}$ , reaction force on the side  $F_S$  and friction force on the side  $F_{\mu S}$ , their changes during the critical spool in the crossover of the rope from one layer to another

are visible. The lower rope layer reaction force  $F_R$  has the steady increasing character from the beginning to the end of the critical spooling, and transcends the nominal value of the pulling force almost by two.

The friction force between the layers  $F_{\mu R}$  also has the increasing character from the beginning of the critical spooling and all the way to the point when the rope crosses to the general spooling case, for it is directly related to the force  $F_R$  by the friction coefficient  $\mu_2$ , (12). The reaction force on the side of the drum  $F_S$  rises up to the spooling angle of  $\varphi \approx 1,5$  [rad], while after reaching the extreme value it decreases to zero. Its value equals zero at  $\varphi \approx 4, 2$  [rad]. The friction force on the side  $F_{\mu S}$  acts similarly, because it is related to the reaction force on the side through the friction coefficient  $\mu_1$ , (12). When the forces  $F_{\mu S}$  and  $F_S$  reach zero, the perpendicular force transfers to the last spool of the lower spooling layer exclusively by the friction force between the rope windings.

### 3.3 General case of rope spooling

General case of rope spooling for multilayered spooling has the greatest share in the spooling process. Generally, friction force occurs on the two rope inlets on the contact line of the winding being spooled and the two spools from the previous layer. In this case the total friction force is divided into two equal parts, (8). Friction force  $F_{\mu LC}$  in line contact on the rope inlet gets close asymptotically to the half of the nominal value of the pulling force, (Fig. 7). In the case of rope spooling onto the higher layers, the general case, in difference with first layer spooling, the friction force carries the total tractive force ( $\varphi \approx 12 \div 15$  [rad]) between the second and the third layer.

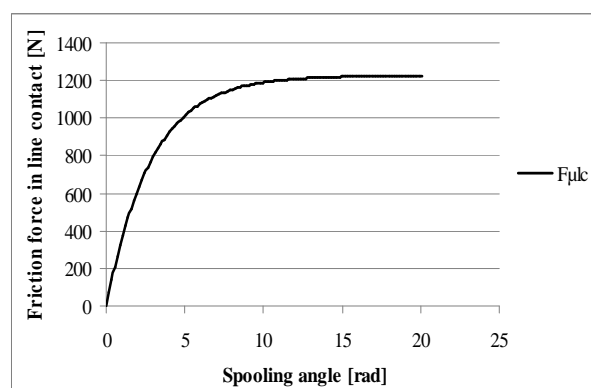


**Fig. 7.** Friction force  $F_{\mu}$  in general case of rope spooling dependence on the spooling angle.

In this case a greater friction coefficient value is adopted from the one used for rope spooling onto the first layer ( $\mu_2=0,35$ ).

### 3.4 Comparative diagrams for different friction coefficient values

Lastly the comparative friction force diagrams (Fig. 8) and perpendicular force (Fig. 9) diagrams for friction coefficients  $\mu = 0,2 \div 0,4$  (initial parameters are also taken from Table 1) are given. For these resulting diagrams the general rope spooling case was used.

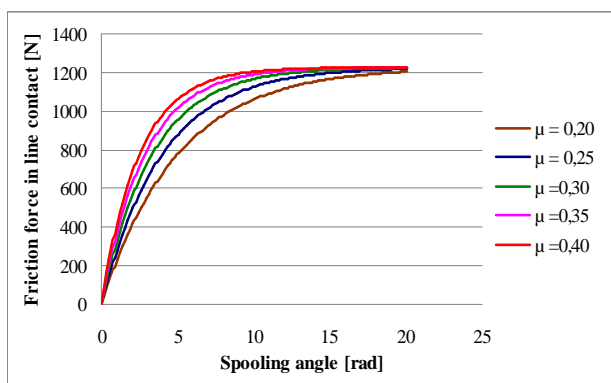


**Fig. 8.** Friction force  $F_\mu$  for different friction coefficients dependence on the spooling angle.

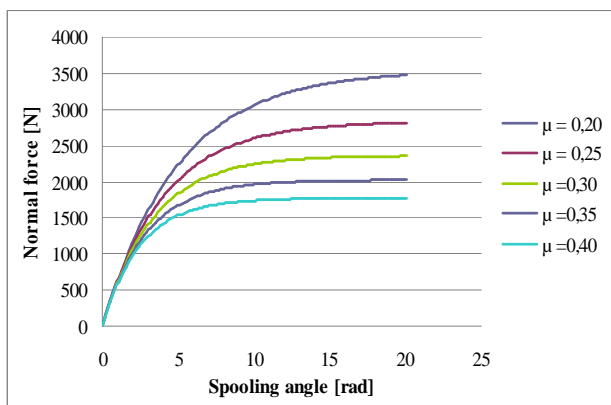


**Fig. 9.** Perpendicular force  $F_N$  for different friction coefficients dependence on spooling angle.

It can be seen from Fig. 8 that for all friction coefficient values the friction force has the same initial value during spooling. As expected, the highest number of spools for total transfer of pulling force to friction force is necessary for the highest friction coefficient ( $\varphi > 12$  [rad]), while for the lowest friction coefficient the transfer is possible only after the third spooling ( $\varphi > 19$  [rad]).

With perpendicular forces the case is slightly different (Fig. 9). Perpendicular forces do not

exceed the nominal value of the pulling force for the value of the friction coefficient of  $\mu < 0,3$ . Perpendicular forces with the friction coefficient of  $\mu < 0,3$  do exceed the value of nominal pulling force.

Even though the perpendicular and friction forces are in linear correlation by the friction coefficient, the differences in their behaviour occur in the general spooling case because the friction force is distributed to the two components on the rope inlets.

## 4. CONCLUSION

Using the mathematical model and friction force calculation, it has been shown that the friction force in the rope spooling onto the winch drum process does not depend only on the friction coefficient, but also in the position of the rope during the process. It has been shown that the greatest friction forces occur during the crossing of the rope from one layer to another. With the increase of the friction coefficient, the time needed for the pulling to friction force transfer shortens. For the transfer with a friction coefficient of 0.2 more than four spools are required ( $\varphi > 24$  [rad]), while for the transfer of the same pulling force with a coefficient of 0.3 less than three spools are needed ( $\varphi < 18$  [rad]).

The friction coefficient value depends mostly on the rope material as well as on its characteristics, but for the first layer the material and the characteristics of the drum have an equal share. For the transfer of smaller masses, ropes with a high friction coefficient can be used, but this is not advisable for greater masses.

During the crossing of the rope from one layer to another, effect of the rope on the side of the drum in the interval when the spooling angle is  $0 < \varphi < 3\pi/2$ , can be seen. Decreasing this force is possible by making a special rope guide. However, this would only solve the problem for the crossing from the first to the second layer.

Further research on this topic could be focused on creating a mathematical model for spooling and an algorithm for determining forces. Experimental research could ensue on models, as well as on actual winches.

## REFERENCES

- [1] P. Yu-xing, Z. Zhen-cai, C. Guo-an, C. Guo-hua: *Effect of Tension on Friction Coefficient Between Lining and Wire Rope with Low Speed Sliding*, Journal of China University of Mining & Technology, Vol. 17, No. 3, pp. 409-413, 2007.
- [2] G. Rebel, M. Borellot, H.D. Chandler: *On the torsional behaviour of triangular-strand hoisting rope*, The Journal of The South African Institute of Mining and Metallurgy, Vol. 38, pp. 279-287, 1996.
- [3] I. Argatov: *International Journal of Solids and Structures*, International Journal of Solids and Structures, Vol. 48, pp. 1413-1423, 2011.
- [4] Y. Wang, B. Wei, X. Wu: *Wet Friction-Elements Boundary Friction Mechanism and Friction Coefficient Prediction*, Tribology in Industry, Vol. 34, No. 4, pp. 198-205, 2012.
- [5] M.A. Chowdhury, D.M. Nuruzzaman, A.H. Mia, M.L. Rahaman: *Friction Coefficient of Different Material Pairs Under Different Normal Loads and Sliding Velocities*, Tribology in Industry, Vol. 34, No. 1, pp. 18-23, 2012.
- [6] S. Babu, K. Manisekar, M.S. Starvin: *Experimental Investigation of Friction Effect on Liner Model Rolling Bearings for Large Diameter Thrust Bearing Design*, Tribology in Industry, Vol. 34, No. 3, pp. 111-118, 2012.
- [7] C.R. Chaplin: *Interactive Fatigue in Wire Rope Applications*, The University of Reading, Reading RG6 6AY, UK, 2008.
- [8] C.R. CHAPLIN: *Failure mechanisms in wire ropes*, Engineering Failure Analysis, Vol. 2, No. 1, pp. 45-57, 1995.
- [9] S.R. Ghoreishi, P. Cartraud, P. Davies, T. Messenger: *Analytical modeling of synthetic fiber ropes subjected to axial loads. Part I: A new continuum model for multilayered fibrous structures*, International Journal of Solids and Structures, Vol. 44, pp. 2924-2942, 2007.
- [10] M. Matejić: *Calculation and design of ship winch in CAD software*, Master thesis, Faculty of engineering science, University in Kragujevac, Kragujevac, 2012.
- [11] B. Simiić: *Design and analysis of ship winch in CAD software*, Master thesis, Faculty of engineering science, University in Kragujevac, Kragujevac, 2012.
- [12] A.K. Moe: *Design consideration of winch*, Master thesis, National University of Singapore, Singapore, 2006.
- [13] L.B. Teck: *Improvement in the design of winches*, Bachelor thesis, National University of Singapore, Singapore, 2005.
- [14] L. Liu, H. Liu: *Study on Optimization Design of a Hoist Roller*, Advanced Materials Research, Vol. 415-417, pp. 460-463, 2012.